Journal of Advanced Research in Fluid Mechanics and Thermal Sciences

Journal homepage:
https://semarakilmu.com.my/journals/index.php/fluid_mechanics_thermal_sciences/index
ISSN: 2289-7879

Sensitivity Analysis of MHD Hybrid Nanofluid Flow over a Radially Shrinking Disk with Heat Generation

Najiyah Safwa Khashi'ie[1,*], Mohd Fariduddin Mukhtar[1], Nurul Amira Zainal[1], Khairum Hamzah[2], Iskandar Waini[2], Abdul Rahman Mohd Kasim[3], Ioan Pop[4]

1 Fakulti Teknologi dan Kejuruteraan Mekanikal, Universiti Teknikal Malaysia Melaka, Hang Tuah Jaya, 76100 Durian Tunggal, Melaka, Malaysia
2 Fakulti Teknologi dan Kejuruteraan Industri dan Pembuatan, Universiti Teknikal Malaysia Melaka, Hang Tuah Jaya, 76100 Durian Tunggal, Melaka, Malaysia
3 Centre for Mathematical Sciences, Universiti Malaysia Pahang Al-Sultan Abdullah, Gambang, 26300 Kuantan, Pahang, Malaysia
4 Department of Mathematics, Babeş-Bolyai University, R-400084 Cluj-Napoca, Romania

ARTICLE INFO

Article history:
Received 5 December 2023
Received in revised form 28 April 2024
Accepted 10 May 2024
Available online 30 May 2024

Keywords:
Dual solutions; hybrid nanofluid; heat generation; magnetic field; response surface analysis; sensitivity analysis; shrinking surface

ABSTRACT

This work features the numerical computation and statistical analysis (response surface and sensitivity) for the flow and thermal progress of an axisymmetric copper-alumina/water hybrid nanofluid subjected to a permeable shrinking disk. The simultaneous factors of magnetic field (MHD), heat generation and suction parameter in the heat transfer development and flow characteristic are observed. The flow and energy equations are mathematically developed based on the boundary layer assumptions. These equations are then simplified with the aids of the similarity variables. The numerical results are then generated by the bvp4c solver in the Matlab software. The dual solutions are possible and exist up to a separation value upon the inclusion of suction effect. The increment of heat generation parameter from 0% to 1% reduces the heat transfer rate for all values of the stretching/shrinking parameter. For the response surface analysis, the responses (skin friction coefficient and heat transfer rate) are analyzed for three factors (magnetic, suction, heat generation) and three magnitudes (low, medium, high). Based on this analysis, the magnetic and suction parameters provide a significant effect on the skin friction with p-values < 0.05. Meanwhile, for the heat transfer coefficient, all factors give significant impact with zero p-values. Meanwhile, the sensitivity analysis reveals that the suction parameter has higher sensitivity to the heat transfer as compared to the magnetic and heat generation parameter. Even though these parameters being less sensitive, their influence on heat transfer remains statistically significant.

1. Introduction

Nanofluids and their characterization, preparation, application and modeling have been the subject of extensive research over the last several decades. Choi and Eastman [1] are credited for developing nanofluid with the theory that adding nanoparticles can improve the heat transmission capabilities of a carrier fluid. Kodi *et al.,* [2] analyzed the heat and mass transfer of non-Newtonian

* *Corresponding author.*
E-mail address: najiyah@utem.edu.my

https://doi.org/10.37934/arfmts.117.2.116130

Jeffrey nanofluid (Cu–water and TiO_2–water) with magnetic field, chemical reaction and radiation effects. They found that the nanoparticles significantly improved the heat transfer process. Other recent studies related to the non-Newtonian nanofluid flow could be found in Kodi *et al.,* [3-6], Vaddemani *et al.,* [7], Kommaddi *et al.,* [8] and Suresh Kumar *et al.,* [9]. Rafique *et al.,* [10] reported the increment of heat transfer rate by 1.135% for single walled carbon nanotubes (SWCNTs) and 1.275% for multi walled carbon nanotubes (MWCNTs) with the application of suction parameter. Meanwhile, Mahmood *et al.,* [11] analyzed and compared the stagnation point flow of nanofluid with SWCNTs and MWCNTs nanoparticles subjected to a stretching surface with the presence of magnetic field and nonlinear thermal radiation. Other works regarding the boundary layer flow of nanofluids could be referred to the previous studies [12-15].

Meanwhile, hybrid and ternary hybrid nanofluids are the most recent nanofluid types created by combining two and three nanoparticles, respectively in a carrier fluid either with or without the appropriate stabilization procedures. The utilization of hybrid nanofluids is based on the core idea of significantly improving the heat transmission, thermophysical and hydrodynamic properties [16]. In applications including automotive, refrigeration, solar energy, air conditioning, biomedical and coolant in manufacturing, hybrid nanofluids are anticipated to perform better than single nanofluids [17,18]. Even though hybrid nanofluids are said to have better heat transfer capability in the majority of situations, further research is still necessary [19]. The recent fundamental and numerical studies of BLF concerning the use of hybrid nanofluids were conducted by Wahid *et al.,* [20], Mousavi *et al.,* [21,22], Khashi'ie *et al.,* [23-26], Mahmood *et al.,* [27] and Rafique *et al.,* [28]. For the surface criteria, a stretching sheet typically enables a viable boundary layer solution as it naturally induces suction towards the surface, facilitating the flow. Adversely, the use of suction through the shrinking surface physically will maintain the opposing fluid movement by stabilizing the vorticity within the boundary layer. From the mathematical view, this parameter will contribute to the generation of multiple solutions when considering shrinking surface.

In addition to numerical interpretations, employing an experimental design in research offers numerous advantages, especially when dealing with multiple factors or parameters and their corresponding outcomes (responses). One commonly used design type is Response Surface Methodology (RSM), which is utilized for analyzing and modeling processes where the response is influenced by various variables. The methodology aims to determine the interaction effects among independent variables. Mehmood *et al.,* [29] discussed the use of ANOVA and RSM for the rotating disk case. Recently, Yahaya *et al.,* [30] used RSM to correlate the heat transfer rate with the testing parameters and found that the suction parameter has a positive impact on this coefficient. Furthermore, RSM and statistical data analysis have been applied to various fluid flow problems, as discussed in previous studies [31-33].

Therefore, the main objective of the present study is to use both numerical and statistical analysis (response surface analysis and sensitivity analysis) in analyzing the significant parameters (magnetic, suction and heat generation) which are used in the present boundary layer flow problem. In order to accomplish this goal, the governing model is first transformed using the similarity transformation into a set of ODEs. Then, the bvp4c solver in the Matlab software is used to solve the ODEs and calculate the responses (skin friction coefficient, heat transfer coefficient). Meanwhile, the central composite design (CCD) in the Minitab software is selected to create the response surface design (RSD) and then analyze the selected numerical data using the ANOVA in the response surface analysis (RSA). By considering three physical factors, a fitted model for each responses are produced based on the statistical data analysis. Besides, by applying the response surface analysis as well as the sensitivity analysis, we can know which parameters are beneficial for the skin friction and heat transfer rate. This analysis is also important to justify the reliability of the present data from a statistical method perspective. Meanwhile, from the numerical method perspective, it is proven that the present data is in accordance with the previous finding as presented in the validation table. Hence, it is best to analyze the present model and data using both statistical and numerical methods. Since no other study of this kind has been done, the novelty and importance of this work are justified. This study will draw a large audience of readers and scholars interested in advancing this research issue because it contributes to the exploration of both statistical data analysis and numerical solutions.

2. Mathematical Formulation

The present investigation highlights a two-dimensional and axisymmetric flow of an incompressible hybrid nanofluid Cu-Al_2O_3/H_2O with magnetic field and heat generation effects. The cylindrical polar coordinate (r, z) is considered where $z-$axis is normal to the sheet while $r-$axis refers to the direction of the flow. The opposing fluid motion is generated due to a shrinking disk (with velocity $\lambda u_w = \lambda cr$; $\lambda < 0$ for shrinking and $\lambda > 0$ for stretching) as depicted in Figure 1. Several assumptions are also considered in this analysis

i. B_0 is the constant which represents magnetic field strength which is directed perpendicular to the sheet.
ii. Q_0 is the constant which represents imposed heat generation effect.
iii. T_w and T_∞ are the respective surface and ambient temperatures.
iv. $v_w = -2S\sqrt{c\nu_f}$ denotes the permeable disk's mass flux velocity with $S > 0$ indicating the suction impact.

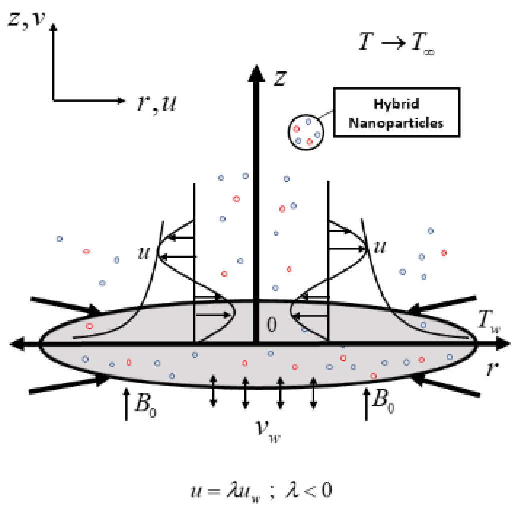

Fig. 1. Illustration of the physical problem with coordinate system

Hence the governing model in PDEs form is [23]

$$\frac{\partial}{\partial r}(ru) + \frac{\partial}{\partial z}(rv) = 0, \tag{1}$$

$$u\frac{\partial u}{\partial r} + v\frac{\partial u}{\partial z} = \frac{\mu_{hnf}}{\rho_{hnf}}\frac{\partial^2 u}{\partial z^2} - \frac{\sigma_{hnf}}{\rho_{hnf}}B_0^{\,2}u, \tag{2}$$

$$u\frac{\partial T}{\partial r}+v\frac{\partial T}{\partial z}=\frac{k_{hnf}}{\left(\rho C_p\right)_{hnf}}\frac{\partial^2 T}{\partial z^2}+\frac{Q_0}{\left(\rho C_p\right)_{hnf}}\left(T-T_\infty\right), \tag{3}$$

$$\left.\begin{array}{l} u=\lambda u_w,\ v=v_w,\ T=T_w \quad \text{at} \quad z=0 \\ u\to 0, \quad T\to T_\infty \quad \text{as} \quad z\to\infty \end{array}\right\}. \tag{4}$$

The velocities in these equations are u and v while T denotes temperature. To simplify the system of differential Eq. (2) to Eq. (4), the following similarity transformation is applied subject to the fulfillment of Eq. (1),

$$\psi=-r^2\sqrt{c\nu_f}\,f\left(\eta\right),\quad \theta\left(\eta\right)=\frac{T-T_\infty}{T_w-T_\infty},\quad \eta=z\sqrt{\frac{c}{\nu_f}}. \tag{5}$$

Here, ψ denotes the stream function with $u=-\frac{1}{r}\frac{\partial\psi}{\partial z}=crf'(\eta)$ and $v=\frac{1}{r}\frac{\partial\psi}{\partial r}=-2\sqrt{c\nu_f}\,f\left(\eta\right)$. Upon the similarity transformation, the Eq. (2) to Eq. (4) are reduced as highlighted in previous study [23]

$$\frac{\mu_{hnf}/\mu_f}{\rho_{hnf}/\rho_{hnf}}f'''+2ff''-f'^2-\frac{\sigma_{hnf}/\sigma_f}{\rho_{hnf}/\rho_{hnf}}Mf'=0, \tag{6}$$

$$\frac{1}{\Pr}\frac{k_{hnf}/k_f}{\left(\rho C_p\right)_{hnf}/\left(\rho C_p\right)_f}\theta''+\frac{Q}{\left(\rho C_p\right)_{hnf}/\left(\rho C_p\right)_f}\theta+2f\theta'=0, \tag{7}$$

$$\begin{array}{l} f(0)=S, \quad f'(0)=\lambda, \quad \theta(0)=1 \\ f'(\eta)\to 0, \quad \theta(\eta)\to 0 \quad \text{as} \quad \eta\to\infty \end{array} \tag{8}$$

where the parameters in Eq. (6) to Eq. (8) are defined as

i. magnetic parameter $\left(M=\frac{\sigma_f B_0^2}{c\rho_f}\right)$;
ii. heat generation parameter $\left(Q=Q_0/\left(\rho C_p\right)_f c\right)$, $Q<0$ for the heat absorption process and $Q>0$ for the heat generation process, and
iii. Prandtl number $\left(\Pr=\left(C_p\mu\right)_f/k_f\right)$; for the computational analysis, $\Pr=6.2$ is used for the water-based fluid.

Table 1 displays the experimentally validated correlations of properties for hybrid nanofluids, as presented by Takabi and Salehi [34]. These correlations are established based on physical assumptions and are applicable for both experimental and numerical investigations. Table 2 lists the specific properties to facilitate computational analysis. These properties serve as inputs for the modeling and simulation of hybrid nanofluid behavior.

Table 1
Correlations of hybrid nanofluid

Properties	Hybrid Nanofluid
Dynamic Viscocity	$\mu_{hnf}=\frac{\mu_f}{\left(1-\phi_{hnf}\right)^{2.5}},\quad \phi_{hnf}=\phi_1+\phi_2$
Heat Capacity	$\left(\rho C_p\right)_{hnf}=\phi_1\left(\rho C_p\right)_{s1}+\phi_2\left(\rho C_p\right)_{s2}+\left(1-\phi_{hnf}\right)\left(\rho C_p\right)_f$
Electrical Conductivity	$\sigma_{hnf}=\left[\frac{\left(\frac{\phi_1\sigma_1+\phi_2\sigma_2}{\phi_{hnf}}\right)-2\phi_{hnf}\sigma_f+2\left(\phi_1\sigma_1+\phi_2\sigma_2\right)+2\sigma_f}{\left(\frac{\phi_1\sigma_1+\phi_2\sigma_2}{\phi_{hnf}}\right)+\phi_{hnf}\sigma_f-\left(\phi_1\sigma_1+\phi_2\sigma_2\right)+2\sigma_f}\right]\sigma_f$
Thermal Conductivity	$k_{hnf}=\left[\frac{\left(\frac{\phi_1 k_1+\phi_2 k_2}{\phi_{hnf}}\right)-2\phi_{hnf}k_f+2\left(\phi_1 k_1+\phi_2 k_2\right)+2k_f}{\left(\frac{\phi_1 k_1+\phi_2 k_2}{\phi_{hnf}}\right)+\phi_{hnf}k_f-\left(\phi_1 k_1+\phi_2 k_2\right)+2k_f}\right]k_f$
Density	$\rho_{hnf}=\phi_1\rho_{s1}+\phi_2\rho_{s2}+\left(1-\phi_{hnf}\right)\rho_f$

Table 2
Thermophysical properties for Cu, H_2O and Al_2O_3

Thermophysical Properties	Cu	H_2O	Al_2O_3
ρ (kg/m^3)	8933	997.1	3970
k (W/mK)	400	0.6130	40
σ(S/m)	59.6 x 10^6	0.05	35 x 10^6
C_p (J/kgK)	385	4179	765

Following Khashi'ie *et al.,* [23], the physical quantities of interest are the skin friction coefficient and thermal transfer rate which are respectively given as

$$0.5\mathrm{Re}_r^{1/2}C_f=\frac{\mu_{hnf}}{\mu_f}f''(0),\qquad \mathrm{Re}_r^{-1/2}Nu_r=-\frac{k_{hnf}}{k_f}\theta'(0) \tag{9}$$

where $\mathrm{Re}_x=ru_w/\nu_f$ denotes the local Reynolds number.

3. Results and Discussion

The function bvp4c in Matlab software is used to compute the numerical solutions for the reduced ODEs in the previous section. The coefficients of heat transfer and skin friction of Cu-Al_2O_3/H_2O are computed within the specific conditions as highlighted in the present figures and tables. Meanwhile, for the optimization through RSM (see next section), three parameters namely magnetic, heat generation and suction are varied for three testing values (low, medium and high magnitudes). The present calculation data is similar to the previously published results which affirm the validity of the present model as displayed in Table 3. However, the slight differences of results in

Case 2 are due to the different use of the hybrid nanofluid's correlations (present-Takabi and Salehi [34], Khashi'ie *et al.,* [23], Devi and Devi [35]).

Table 3
Model validation of $f''(0)$ when $\lambda = 1$ and $Q = 0$

M	Case 1 ($\phi_1 = \phi_2 = 0,\ \Pr = 1$)			Case 2 ($\phi_1 = 0.1,\ \phi_2 = 0.05,\ \Pr = 6.2$)		
	Present	Khashi'ie *et al.,* [23]	Soid *et al.,* [36]	Present	Khashi'ie *et al.,* [23]	Soid *et al.,* [36]
0.0	-1.17372	-1.17372	-1.17372	-1.24757	−1.25121	−
0.5	-1.36581	-1.36581	-1.36581	-1.43286	−1.44026	−
1.0	-1.53571	-1.53571	-1.53571	-1.59836	−1.60883	−
2.0	-1.83049	-1.83049	-1.83049	-1.88806	−1.90345	−
3.0	-2.08485	-2.08485	-2.08485	-2.13980	−2.15915	−

This section also highlights the reverse flow of hybrid nanofluid caused by the shrinking disk. The unrestrained vorticity of this opposing flow can be stabilized using the application of suction. Figure 2 shows the existence of two boundary layer solutions up to a separation value $\lambda_c = -2.5138$. The heat generation parameter is not directly affecting the fluid motion and as a consequence, the separation value as well as the skin friction coefficient remains unchanged with the increment of Q. Meanwhile, the thermal rate shows a downward trend as Q increased from 0% to 1%. Another observation is the thermal rate slightly increases as $\lambda \to +\lambda$ due to the aiding flow. The higher value of the shrinking parameter $(\lambda \to -\lambda)$ reflects the restriction in fluid motion due to the unconfined vorticity in the opposing shrinking flow.

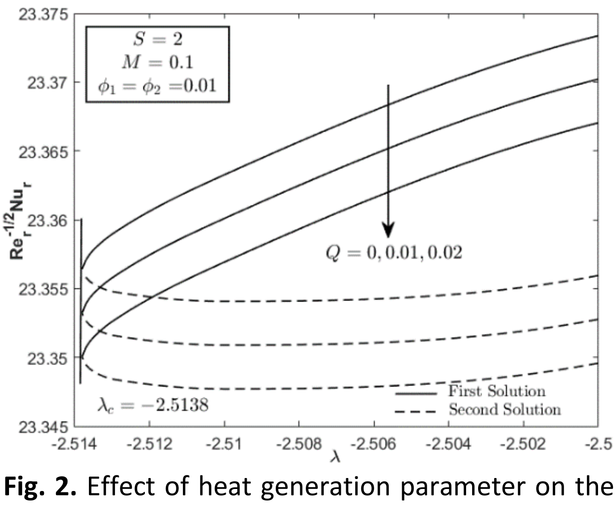

Fig. 2. Effect of heat generation parameter on the heat transfer coefficient rate

4. Response Surface Analysis

The Response Surface Methodology (RSM) is important in designing an experiment with more than two factors/parameters to identify the factor settings which optimize the responses (skin friction coefficient, thermal rate) including to develop a model for the curvature in the data. In Table 3, the RSM which employs the central composite design with 3 factors and 20 runs is highlighted. The magnetic, suction, and heat generation parameters are denoted as A, B and C, respectively. These factors are classified into low (-1), medium (0), and high (+1) levels to represent their magnitudes. There are no specific criteria in selecting the three testing values (low, medium, high) of each parameter. The values are based on the possibility of the numerical solutions for the shrinking flow case in which the first solution being the responses. For the RSM, the total number of runs follows the formula of $R = C + 2k + 2^k$ such that C, $2k$ and 2^k denotes the center points, axial points and factorial/cube points, respectively. In this study, $k = 3$ and $C = 6$ are used. Table 4 is generated based on the response surface design proposed by the Minitab software. From Table 3, a general response surface Eq. (10) can also be computed:

$$y = r_0 + r_{\mathrm{A}}\mathrm{A} + r_{\mathrm{B}}\mathrm{B} + r_{\mathrm{C}}\mathrm{C} + r_{\mathrm{AB}}\mathrm{AB} + r_{\mathrm{CA}}\mathrm{CA} + r_{\mathrm{BC}}\mathrm{BC} + r_{\mathrm{A}^2}\mathrm{A}^2 + r_{\mathrm{B}^2}\mathrm{B}^2 + r_{\mathrm{C}^2}\mathrm{C}^2 + \varepsilon \tag{10}$$

Table 4
RSM for the case of $\phi_1 = \phi_2 = 0.01$, $\mathrm{Pr} = 6.2$ and $\lambda = -2.5$

Run	Real			Coded			Responses	
	M	S	Q	A	B	C	$0.5\mathrm{Re}_r^{1/2}C_f$	$\mathrm{Re}_r^{-1/2}Nu_r$
1	0.15	2.1	0.01	0	0	0	8.313513970	24.708231236
2	0.15	2.1	0.01	0	0	0	8.313513970	24.708231236
3	0.1	2.2	0.02	-1	1	1	9.173952956	26.013594846
4	0.1	2.2	0	-1	1	-1	9.173952956	26.019099367
5	0.2	2.1	0.01	1	0	0	8.396228092	24.710024214
6	0.1	2	0.02	-1	-1	1	6.766644775	23.367045065
7	0.15	2	0.01	0	-1	0	7.030725864	23.377304847
8	0.15	2.1	0.01	0	0	0	8.313513970	24.708231236
9	0.2	2	0.02	1	-1	1	7.212474145	23.378951253
10	0.1	2	0	-1	-1	-1	6.766644776	23.373376578
11	0.15	2.1	0	0	0	-1	8.313513970	24.711165307
12	0.15	2.2	0.01	0	1	0	9.237377733	26.017528909
13	0.15	2.1	0.02	0	0	1	8.313513970	24.705296321
14	0.15	2.1	0.01	0	0	0	8.313513970	24.708231236
15	0.2	2.2	0.02	1	1	1	9.299221234	26.015926350
16	0.1	2.1	0.01	-1	0	0	8.226710821	24.706340906
17	0.15	2.1	0.01	0	0	0	8.313513970	24.708231236
18	0.2	2.2	0	1	1	-1	9.299221234	26.021428155
19	0.15	2.1	0.01	0	0	0	8.313513970	24.708231236
20	0.2	2	0	1	-1	-1	7.212474145	23.385262421

Prior to further analysis, it is crucial to assess the normality distribution of each response before carrying the ANOVA tests. Figure 3 and Figure 4 present normality plots for skin friction and heat transfer, respectively using the data in Table 3. In both cases, the distributions closely align with the normal line as can be seen in Figure 3(a) and Figure 4(a). In addition, the histogram results (see Figure 3(b) and Figure 4(b)) reveal a low mean value, approximating zero, indicating the ideal nature of the distributions. Additionally, the standard deviation reflects satisfactory results regarding the variability of the model error which means that the responses in Table 4 are statistically acceptable.

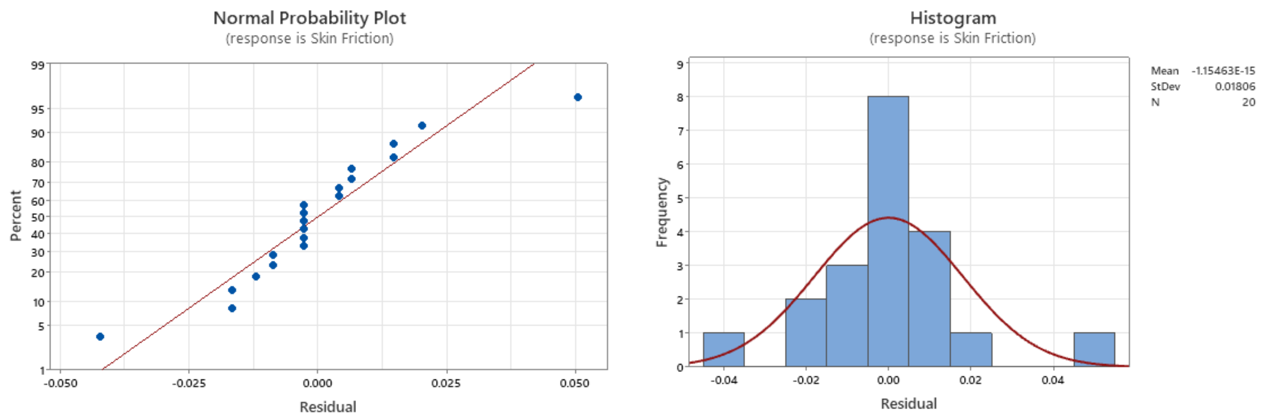

(a) (b)

Fig. 3. Illustrations of (a) normal probability plot, (b) histogram of standardized residual for skin friction

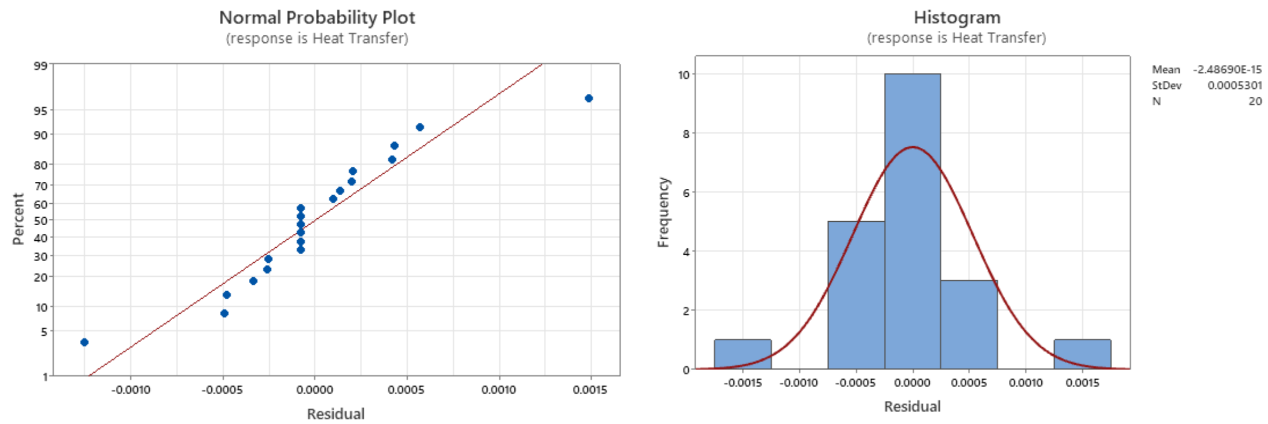

(a) (b)

Fig. 4. Illustrations of (a) normal probability plot, (b) histogram of standardized residual for heat transfer

Table 5 displays the response surface ANOVA analysis, analyzing the effects of A, B, and C and their interactions on the skin friction (response 1) and heat transfer rate (response 2). The factors A and B as well as the interactions AB and BB provide a significant effect on the $0.5\mathrm{Re}_r^{1/2} C_f$ (p-values < 0.05). For the heat transfer coefficient, all single factors give significant impact with zero p-values. Meanwhile, the high value of R-squared (R-sq) and R-sq (adj), 99.95% and 99.91% for the skin friction model indicate that the model fits the data well as featured in Table 4.

In addition, through the response surface analysis, the fitted models are also obtained by considering the effects and its interactions. The fitted models are given in Eq. (11) and Eq. (12) for skin friction and heat transfer respectively.

$$y_{0.5\mathrm{Re}_r^{1/2} C_f} = 8.31627 + 0.13117\mathrm{A} + 1.11948\mathrm{B} - 0.00890\mathrm{A}^2 - 0.18630\mathrm{B}^2 - 0.00690\mathrm{C}^2 - 0.08014\mathrm{AB} \quad (11)$$

$$y_{\mathrm{Re}_r^{-1/2} Nu_r} = 24.7083 + 0.003214\mathrm{A} + 1.32056\mathrm{B} - 0.002952\mathrm{C} - 0.000242\mathrm{A*A} - 0.011008\,\mathrm{B*B} - 0.000194\,\mathrm{C*C} - 0.002391\mathrm{AB} + 0.000003\mathrm{AC} + 0.000205\mathrm{BC} \quad (12)$$

Table 5 reveals the significance of factors A and B in relation to skin friction. To assess the sensitivity of each factor to the skin friction response, a dedicated sensitivity analysis for parameters

A, B, and C is conducted and is presented in Eq. (13). The formulation of this sensitivity analysis is grounded in the derivation of the response function outlined in Eq. (11).

$$\frac{\partial\left(y_{0.5\mathrm{Re}_r^{1/2}C_f}\right)}{\partial \mathrm{A}} = 0.13117 - 0.0178\mathrm{A} - 0.08014\mathrm{B}\ ,$$
$$\frac{\partial\left(y_{0.5\mathrm{Re}_r^{1/2}C_f}\right)}{\partial \mathrm{B}} = 1.11948 - 0.3726\mathrm{B} - 0.08014\mathrm{A}, \tag{13}$$
$$\frac{\partial\left(y_{0.5\mathrm{Re}_r^{1/2}C_f}\right)}{\partial \mathrm{C}} = -0.0138\mathrm{C},$$

Table 5
Statistical analysis result

Source	DF	Adj SS	Adj MS	F-Value	P-Value
Skin friction coefficient					
A	1	0.1721	0.1721	277.79	0.000
B	1	12.5323	12.5323	20233.43	0.000
C	1	0.0000	0.0000	0.00	1.000
A*A	1	0.0002	0.0002	0.35	0.565
B*B	1	0.0955	0.0955	154.18	0.000
C*C	1	0.0001	0.0001	0.21	0.656
A*B	1	0.0514	0.0514	82.95	0.000
A*C	1	0.0000	0.0000	0.00	1.000
B*C	1	0.0000	0.0000	0.00	1.000
Error	10	0.0062	0.0006		
Lack-of-Fit	5	0.0062	0.0012	*	*
Pure Error	5	0.0000	0.0000		
Total	19	12.9542			
R-sq	99.95%	R-sq(adj)	99.91%		
Heat Transfer Coefficient					
A	1	0.0001	0.0001	193.39	0.000
B	1	17.4389	17.4389	32657883.67	0.000
C	1	0.0001	0.0001	163.17	0.000
A*A	1	0.0000	0.0000	0.30	0.595
B*B	1	0.0003	0.0003	624.04	0.000
C*C	1	0.0000	0.0000	0.19	0.669
A*B	1	0.0000	0.0000	85.68	0.000
A*C	1	0.0000	0.0000	0.00	0.991
B*C	1	0.0000	0.0000	0.63	0.447
Error	10	0.0000	0.0000		
Lack-of-Fit	5	0.0000	0.0000	*	*
Pure Error	5	0.0000	0.0000		
Total	19	17.4398			
R-sq	100%	R-sq(adj)	100%		

Figure 5 presents a comparison of the sensitivity analysis for factors A, B, and C concerning skin friction. Longer bars denote higher sensitivity, while shorter bars indicate lower sensitivity. This figure aligns with the ANOVA analysis, confirming that factors A and B are the most sensitive to changes in skin friction. The results suggest that magnetics and suction are the two most influential factors affecting skin friction. Additionally, the contour plot illustrations as in Figure 6 indicate that the interaction between A and B is much more significant than the interaction between C and A.

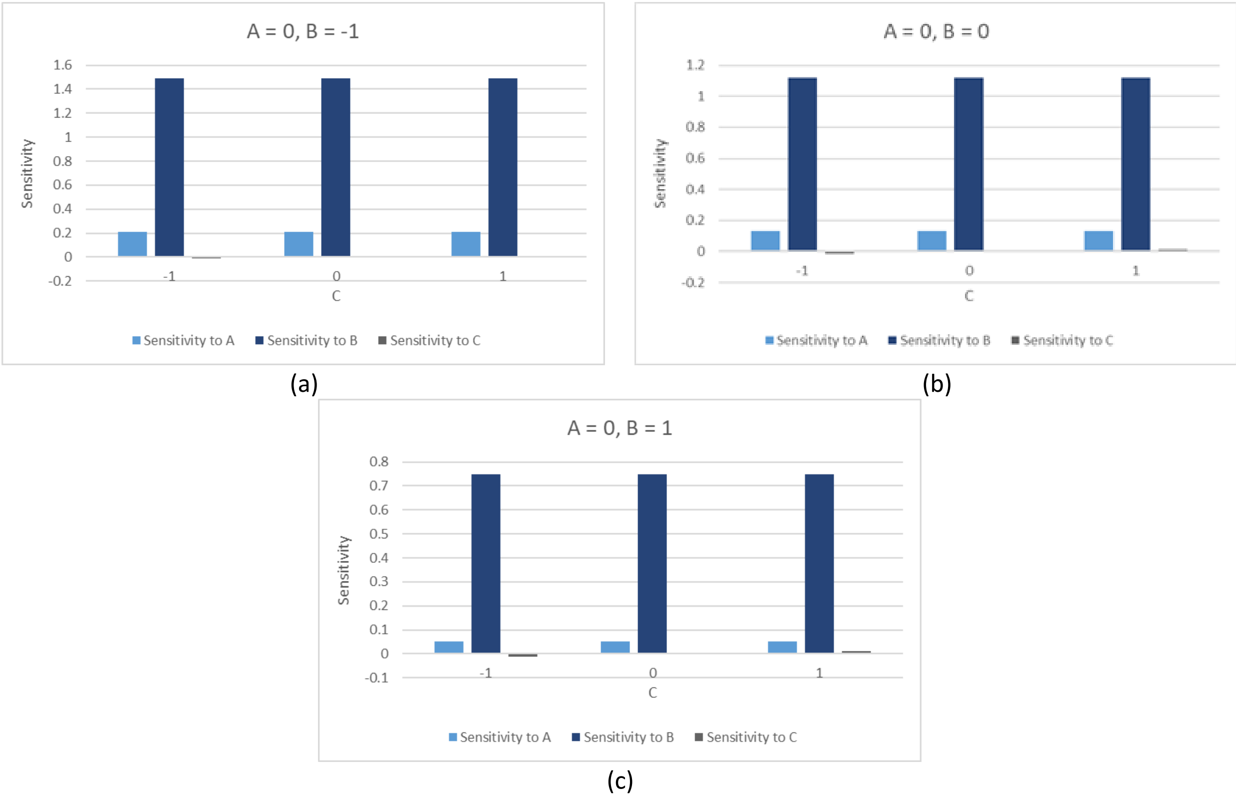

Fig. 5. Illustrations of sensitivity analysis of each variable for (a) A = 0, B = -1, (b) A = 0, B = 0, (c) A = 0, B = 1

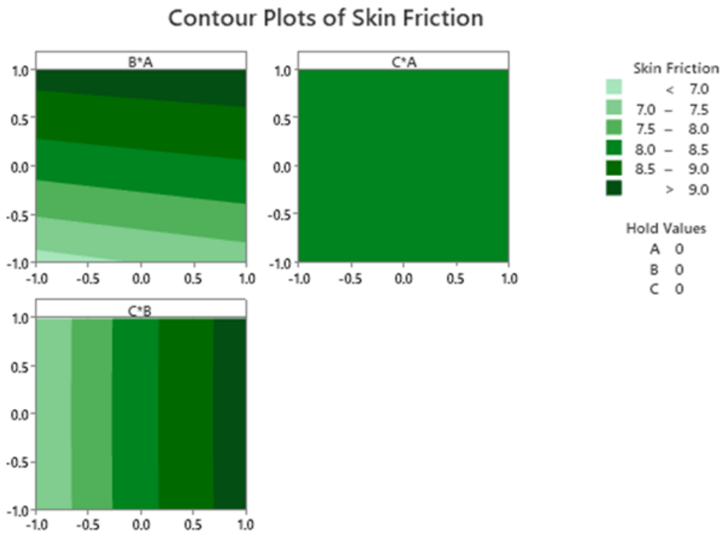

Fig. 6. Sensitivity of responses with combinations of different factors A, B and C

As for the heat transfer, Table 5 shows that factor A, B and C are significant with heat transfer. In order to check the sensitivity of each factor, Eq. (14) was developed as the partial derivatives of the regression's equation in Eq. (13).

$$\frac{\partial\left(y_{\mathrm{Re}_r^{-1/2} Nu_r}\right)}{\partial \mathrm{A}} = 0.003214 - 0.000484\mathrm{A} - 0.002391\mathrm{B} + 0.000003\mathrm{C},$$
$$\frac{\partial\left(y_{\mathrm{Re}_r^{-1/2} Nu_r}\right)}{\partial \mathrm{B}} = 1.32056 - 0.022016\mathrm{B} - 0.002391\mathrm{A} + 0.000205\mathrm{C},$$
$$\frac{\partial\left(y_{\mathrm{Re}_r^{-1/2} Nu_r}\right)}{\partial \mathrm{C}} = -0.002952 - 0.000388\mathrm{C} + 0.000003\mathrm{A} + 0.000205\mathrm{B},$$
(14)

Similarly, a comprehensive sensitivity analysis was undertaken for each factor. Intriguingly, while the ANOVA analysis underscored the significance of each factor in the context of heat transfer, the sensitivity analysis, as depicted in Figure 7, revealed nuanced insights. Notably, suction (Factor B) displayed markedly higher sensitivity to heat transfer compared to magnetic influence (Factor A) and heat generation (Factor C). Despite factors A and C being less sensitive, their influence on heat transfer remains statistically significant.

Upon closer examination of the patterns and trends illustrated by the contour lines and colours in Figure 8, a distinct revelation emerged. The darker colour gradients on the plot denote interactions between two factors, suggesting complex relationships within the system. This observation implies that the interplay among the factors significantly influences the heat transfer dynamics. The detailed examination of these interactions provides a deeper understanding of the system's behaviour, enriching our insights into the intricate relationships governing heat transfer under the influence of the studied factors.

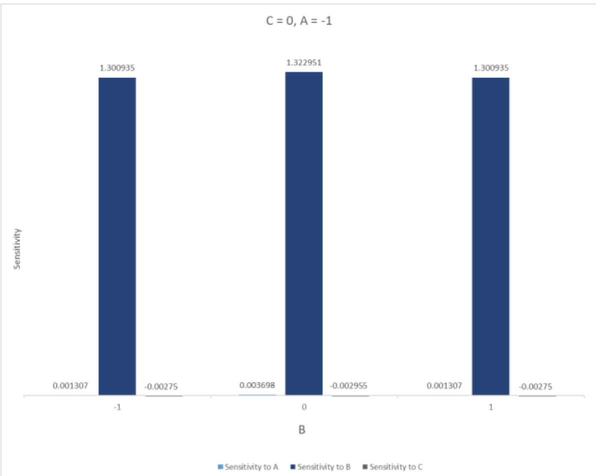

(a)

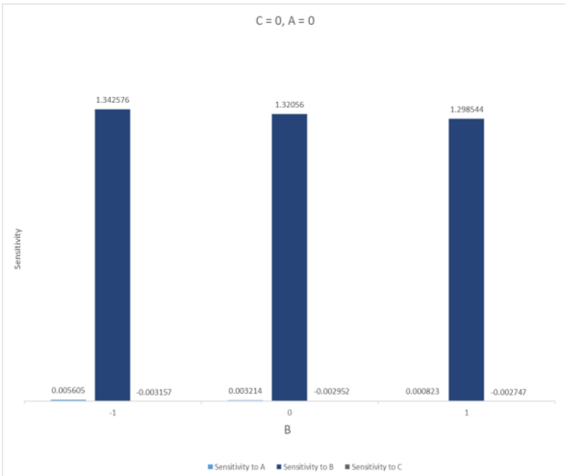

(b)

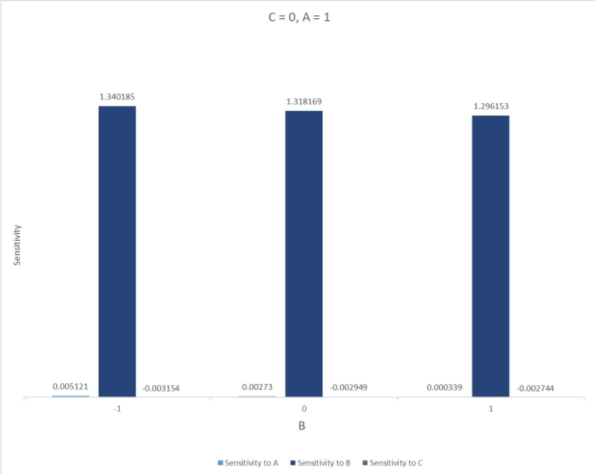

(c)

Fig. 7. Illustrations of sensitivity analysis for each variable for (a) C = 0, A = -1, (b) C = 0, A = 0, (c) C = 0, A = 1

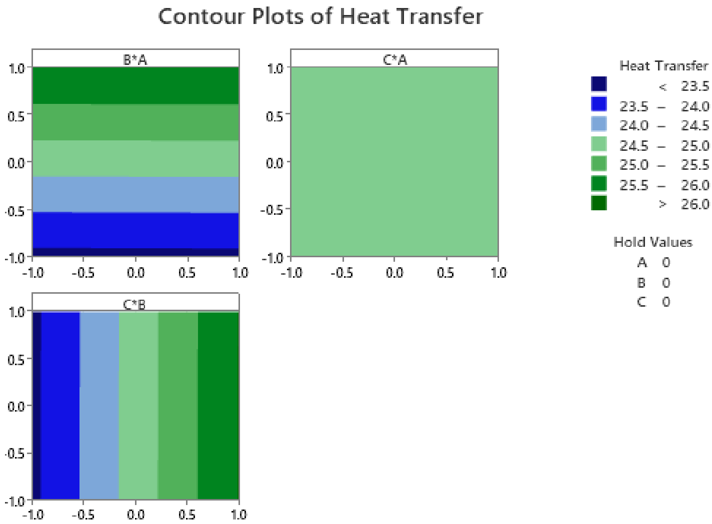

Fig. 8. Sensitivity of responses with combinations of different factors A, B and C

5. Conclusion

This study focuses on investigating the Cu-Al_2O_3/H_2O flow behavior subjected to different factors (magnetic field, suction and heat generation) over a shrinking disk. A similarity transformation is applied, resulting in a set of ODEs. The steady similarity solutions are numerically computed using the bvp4c program. In addition to numerical analysis, RSM is also performed. This approach allows for the examination of the relationship between the input parameters and the responses. To summarize the findings, the details of the study's outcomes are as follows

i. Dual solutions are detected within the specific use of physical factors, however the stable first solution is selected based on the first fulfillment of the far field condition.
ii. Based on the response surface analysis, the magnetic, heat generation and suction parameters are the significant factors for the heat transfer development while the skin friction coefficient is influenced by the magnetic and suction effects.

Acknowledgement
We acknowledge Universiti Teknikal Malaysia Melaka and Ministry of the Higher Education (MoHE-Malaysia) for the grant FRGS/1/2021/STG06/UTEM/03/1.

References

[1] Choi, S. U. S., and Jeffrey A. Eastman. *Enhancing thermal conductivity of fluids with nanoparticles*. No. ANL/MSD/CP-84938; CONF-951135-29. Argonne National Lab.(ANL), Argonne, IL (United States), 1995.
[2] Kodi, Raghunath, Farhan Ali, M. Khalid, Barno Sayfutdinovna Abdullaeva, Reem Altuijri, and M. Ijaz Khan. "Heat and mass transfer on MHD flow of Jeffrey nanofluid based on Cu and TiO_2 over an inclined plate and diffusion-thermo and radiation absorption effects." *Pramana* 97, no. 4 (2023): 202. https://doi.org/10.1007/s12043-023-02673-3
[3] Kodi, Raghunath, Ramachandra Reddy Vaddemani, M. Ijaz Khan, Sherzod Shukhratovich Abdullaev, Attia Boudjemline, Mohamed Boujelbene, and Yassine Bouazzi. "Unsteady magneto-hydro-dynamics flow of Jeffrey fluid through porous media with thermal radiation, Hall current and Soret effects." *Journal of Magnetism and Magnetic Materials* 582 (2023): 171033. https://doi.org/10.1016/j.jmmm.2023.171033
[4] Kodi, Raghunath, Charankumar Ganteda, Abhishek Dasore, M. Logesh Kumar, G. Laxmaiah, Mohd Abul Hasan, Saiful Islam, and Abdul Razak. "Influence of MHD mixed convection flow for maxwell nanofluid through a vertical cone with porous material in the existence of variable heat conductivity and diffusion." *Case Studies in Thermal Engineering* 44 (2023): 102875. https://doi.org/10.1016/j.csite.2023.102875
[5] Kodi, Raghunath, Ravuri Mohana Ramana, Charankumar Ganteda, Prem Kumar Chaurasiya, Damodar Tiwari, Rajan Kumar, Dharam Buddhi, and Kuldeep Kumar Saxena. "Processing to pass unsteady MHD flow of a second-grade fluid through a porous medium in the presence of radiation absorption exhibits Diffusion thermo, hall and ion slip effects." *Advances in Materials and Processing Technologies* (2023): 1-18. https://doi.org/10.1080/2374068X.2023.2191450
[6] Kodi, Raghunath, R. Mohana Ramana, V. Ramachandra Reddy, and M. Obulesu. "Diffusion Thermo and Chemical Reaction Effects on Magnetohydrodynamic Jeffrey Nanofluid Over an Inclined Vertical Plate in the Presence of Radiation Absorption and Constant Heat Source." *Journal of Nanofluids* 12, no. 1 (2023): 147-156. https://doi.org/10.1166/jon.2023.1923
[7] Vaddemani, Ramachandra Reddy, Sreedhar Ganta, and Raghunath Kodi. "Effects of hall current, activation energy and diffusion thermo of MHD Darcy-Forchheimer Casson nanofluid flow in the presence of Brownian motion and thermophoresis." *Journal of Advanced Research in Fluid Mechanics and Thermal Sciences* 105, no. 2 (2023): 129-145. https://doi.org/10.37934/arfmts.105.2.129145
[8] Kommaddi, Hari Babu, Raghunath Kodi, Charankumar Ganteda, and Giulio Lorenzini. "Heat and Mass Transfer on Unsteady MHD Chemically Reacting Rotating Flow of Jeffrey Fluid Past an Inclined Plates under the Impact of Hall Current, Diffusion Thermo and Radiation Absorption." *Journal of Advanced Research in Fluid Mechanics and Thermal Sciences* 111, no. 2 (2023): 225-241. https://doi.org/10.37934/arfmts.111.2.225241
[9] Suresh Kumar, Y., Shaik Hussain, K. Raghunath, Farhan Ali, Kamel Guedri, Sayed M. Eldin, and M. Ijaz Khan. "Numerical analysis of magnetohydrodynamics Casson nanofluid flow with activation energy, Hall current and thermal radiation." *Scientific Reports* 13, no. 1 (2023): 4021. https://doi.org/10.1038/s41598-023-28379-5
[10] Rafique, Khadija, Zafar Mahmood, Umar Khan, Sayed M. Eldin, and Alia M. Alzubaidi. "Mathematical analysis of radius and length of CNTs on flow of nanofluid over surface with variable viscosity and joule heating." *Heliyon* 9, no. 7 (2023). https://doi.org/10.1016/j.heliyon.2023.e17673
[11] Mahmood, Zafar, Khadija Rafique, Adnan, Umar Khan, Taseer Muhammad, and Ahmed M. Hassan. "MHD unsteady flow of carbon nanotubes over nonlinear radiative surface with anisotropic slip conditions: computational analysis of irreversibility for Yamada-Ota model." *Engineering Applications of Computational Fluid Mechanics* 18, no. 1 (2024): 2309139. https://doi.org/10.1080/19942060.2024.2309139
[12] Khan, Umar, Khadija Rafique, and Zafar Mahmood. "Significance of unsteady rotating flow of nanofluid with nanoparticles aggregation and impacts of slip conditions and variable viscosity." *Numerical Heat Transfer, Part A: Applications* (2023): 1-28. https://doi.org/10.1080/10407782.2023.2299294
[13] Mahmood, Zafar, Khadija Rafique, Umar Khan, Sidra Jubiar, Fuad A. Awwad, and Emad AA Ismail. "Investigation of entropy generation in the existence of heat generation and nanoparticle clustering on porous Riga plate during nanofluid flow." *Materials Today Communications* 38 (2024): 108165. https://doi.org/10.1016/j.mtcomm.2024.108165
[14] Sooppy Nisar, Kottakkaran, Dolat Khan, Arshad Khan, Waqar A. Khan, Ilyas Khan, and Abdullah Mohammed Aldawsari. "Entropy generation and heat transfer in drilling nanoliquids with clay nanoparticles." *Entropy* 21, no. 12 (2019): 1226. https://doi.org/10.3390/e21121226

[15] Khan, Dolat, Poom Kumam, Wiboonsak Watthayu, and Ilyas Khan. "Heat transfer enhancement and entropy generation of two working fluids of MHD flow with titanium alloy nanoparticle in Darcy medium." *Journal of Thermal Analysis and Calorimetry* 147, no. 19 (2022): 10815-10826. https://doi.org/10.1007/s10973-022-11284-w

[16] Babu, J. A. Ranga, K. Kiran Kumar, and S. Srinivasa Rao. "State-of-art review on hybrid nanofluids." *Renewable and Sustainable Energy Reviews* 77 (2017): 551-565. https://doi.org/10.1016/j.rser.2017.04.040

[17] Jamil, Furqan, and Hafiz Muhammad Ali. "Applications of hybrid nanofluids in different fields." In *Hybrid Nanofluids for Convection Heat Transfer*, pp. 215-254. Academic Press, 2020. https://doi.org/10.1016/B978-0-12-819280-1.00006-9

[18] Sidik, Nor Azwadi Che, Isa Muhammad Adamu, Muhammad Mahmud Jamil, G. H. R. Kefayati, Rizalman Mamat, and G. Najafi. "Recent progress on hybrid nanofluids in heat transfer applications: a comprehensive review." *International Communications in Heat and Mass Transfer* 78 (2016): 68-79. https://doi.org/10.1016/j.icheatmasstransfer.2016.08.019

[19] Eshgarf, Hamed, Rasool Kalbasi, Akbar Maleki, Mostafa Safdari Shadloo, and Arash Karimipour. "A review on the properties, preparation, models and stability of hybrid nanofluids to optimize energy consumption." *Journal of Thermal Analysis and Calorimetry* 144 (2021): 1959-1983. https://doi.org/10.1007/s10973-020-09998-w

[20] Wahid, Nur Syahirah, Norihan Md Arifin, Najiyah Safwa Khashi'ie, Ioan Pop, Norfifah Bachok, and Mohd Ezad Hafidz Hafidzuddin. "Unsteady MHD mixed convection flow of a hybrid nanofluid with thermal radiation and convective boundary condition." *Chinese Journal of Physics* 77 (2022): 378-392. https://doi.org/10.1016/j.cjph.2022.03.013

[21] Mousavi, Seyed Mahdi, Mohammadreza Nademi Rostami, Mohammad Yousefi, Saeed Dinarvand, Ioan Pop, and Mikhail A. Sheremet. "Dual solutions for Casson hybrid nanofluid flow due to a stretching/shrinking sheet: A new combination of theoretical and experimental models." *Chinese Journal of Physics* 71 (2021): 574-588. https://doi.org/10.1016/j.cjph.2021.04.004

[22] Mousavi, Seyed Mehdi, Mohammadreza Nademi Rostami, Mohammad Yousefi, and Saeed Dinarvand. "Dual solutions for MHD flow of a water-based TiO_2-Cu hybrid nanofluid over a continuously moving thin needle in presence of thermal radiation." *Reports in Mechanical Engineering* 2, no. 1 (2021): 31-40. https://doi.org/10.31181/rme200102031m

[23] Khashi'ie, Najiyah Safwa, Norihan Md Arifin, Roslinda Nazar, Ezad Hafidz Hafidzuddin, Nadihah Wahi, and Ioan Pop. "Magnetohydrodynamics (MHD) axisymmetric flow and heat transfer of a hybrid nanofluid past a radially permeable stretching/shrinking sheet with Joule heating." *Chinese Journal of Physics* 64 (2020): 251-263. https://doi.org/10.1016/j.cjph.2019.11.008

[24] Khashi'ie, Najiyah Safwa, Norihan Md Arifin, and Ioan Pop. "Unsteady axisymmetric radiative Cu-Al_2O_3/H_2O flow over a radially stretching/shrinking surface." *Chinese Journal of Physics* 78 (2022): 169-179. https://doi.org/10.1016/j.cjph.2022.06.003

[25] Khashi'ie, Najiyah Safwa, Natalia C. Roșca, Alin V. Roșca, and Ioan Pop. "Dual solutions on MHD radiative three-dimensional bidirectional nanofluid flow over a non-linearly permeable shrinking sheet." *Alexandria Engineering Journal* 71 (2023): 401-411. https://doi.org/10.1016/j.aej.2023.03.066

[26] Khashi'ie, Najiyah Safwa, Norihan M. Arifin, John H. Merkin, Rusya Iryanti Yahaya, and Ioan Pop. "Mixed convective stagnation point flow of a hybrid nanofluid toward a vertical cylinder." *International Journal of Numerical Methods for Heat & Fluid Flow* 31, no. 12 (2021): 3689-3710. https://doi.org/10.1108/HFF-11-2020-0725

[27] Mahmood, Zafar, Khadija Rafique, Umar Khan, Magda Abd El-Rahman, and Rabab Alharbi. "Analysis of mixed convective stagnation point flow of hybrid nanofluid over sheet with variable thermal conductivity and slip Conditions: A Model-Based study." *International Journal of Heat and Fluid Flow* 106 (2024): 109296. https://doi.org/10.1016/j.ijheatfluidflow.2024.109296

[28] Rafique, Khadija, Zafar Mahmood, Umar Khan, Sayed M. Eldin, Mowffaq Oreijah, Kamel Guedri, and Hamiden Abd El-Wahed Khalifa. "Investigation of thermal stratification with velocity slip and variable viscosity on MHD flow of Al_2O_3−Cu−TiO_2/H_2O nanofluid over disk." *Case Studies in Thermal Engineering* 49 (2023): 103292. https://doi.org/10.1016/j.csite.2023.103292

[29] Mehmood, Tahir, Muhammad Ramzan, Fares Howari, Seifedine Kadry, and Yu-Ming Chu. "Application of response surface methodology on the nanofluid flow over a rotating disk with autocatalytic chemical reaction and entropy generation optimization." *Scientific Reports* 11, no. 1 (2021): 4021. https://doi.org/10.1038/s41598-021-81755-x

[30] Yahaya, Rusya Iryanti, Mohd Shafie Mustafa, Norihan Md Arifin, Ioan Pop, Fadzilah Md Ali, and Siti Suzilliana Putri Mohamed Isa. "Hybrid nanofluid flow past a biaxial stretching/shrinking permeable surface with radiation effect: Stability analysis and heat transfer optimization." *Chinese Journal of Physics* 85 (2023): 402-420. https://doi.org/10.1016/j.cjph.2023.06.003

[31] Khashi'ie, Najiyah Safwa, Iskandar Waini, Mohd Fariduddin Mukhtar, Nurul Amira Zainal, Khairum Bin Hamzah, Norihan Md Arifin, and Ioan Pop. "Response surface methodology (RSM) on the hybrid nanofluid flow subject to a vertical and permeable wedge." *Nanomaterials* 12, no. 22 (2022): 4016. https://doi.org/10.3390/nano12224016

[32] Hussain, Shahid, Kianat Rasheed, Aamir Ali, Narcisa Vrinceanu, Ahmed Alshehri, and Zahir Shah. "A sensitivity analysis of MHD nanofluid flow across an exponentially stretched surface with non-uniform heat flux by response surface methodology." *Scientific Reports* 12, no. 1 (2022): 18523. https://doi.org/10.1038/s41598-022-22970-y

[33] Khashi'ie, Najiyah Safwa, Iskandar Waini, Khairum Bin Hamzah, Mohd Fariduddin Mukhtar, Abdul Rahman Mohd Kasim, Norihan Md Arifin, and Ioan Pop. "Numerical solution and statistical analysis of the unsteady hybrid ferrofluid flow with heat generation subject to a rotating disk." *ZAMM-Journal of Applied Mathematics and Mechanics/Zeitschrift für Angewandte Mathematik und Mechanik* 103, no. 6 (2023): e202200384. https://doi.org/10.1002/zamm.202200384

[34] Takabi, Behrouz, and Saeed Salehi. "Augmentation of the heat transfer performance of a sinusoidal corrugated enclosure by employing hybrid nanofluid." *Advances in Mechanical Engineering* 6 (2014): 147059. https://doi.org/10.1155/2014/147059

[35] Devi, S. P. Anjali, and S. Suriya Uma Devi. "Numerical investigation of hydromagnetic hybrid Cu-Al_2O_3/water nanofluid flow over a permeable stretching sheet with suction." *International Journal of Nonlinear Sciences and Numerical Simulation* 17, no. 5 (2016): 249-257. https://doi.org/10.1515/ijnsns-2016-0037

[36] Soid, Siti Khuzaimah, Anuar Ishak, and Ioan Pop. "MHD flow and heat transfer over a radially stretching/shrinking disk." *Chinese Journal of Physics* 56, no. 1 (2018): 58-66. https://doi.org/10.1016/j.cjph.2017.11.022